Spanwise Variations in Profile Drag for Airfoils at Low Reynolds Numbers

James J. Guglielmo* and Michael S. Selig†
University of Illinois at Urbana–Champaign, Urbana, Illinois 61801-2935

In a nominally two-dimensional flow, extensive wake surveys were performed on two airfoils at low Reynolds numbers to quantify the profile drag variation along the airfoil model span. Wake profile measurements were made at 57 spanwise stations spaced 2% chord apart and 1.25 chord lengths downstream of the trailing edge. Results at a Reynolds number (Re) of 2×10^5 show that variations on the order of 5–40% are typical. In an extreme case, however, over a spanwise distance of less than 12% chord, the profile drag coefficient changed from approximately 0.006 to 0.016, which illustrates the sometimes rather dramatic three-dimensional nature of the flow. Measurements taken at higher Reynolds numbers and closer to the trailing edge showed significant reductions in the spanwise drag variation, which suggests that the laminar separation bubble and the developing wake play an important role. A zigzag boundary-layer trip and an isolated roughness element were also investigated to examine their effects as compared with their respective undisturbed cases. Finally, the results suggest that the lack of good agreement in profile drag measurements between different wind-tunnel facilities can partly be traced to the associated measurement techniques used as well as the flowfield three dimensionality. Differences in agreement between facilities can be expected when only one spanwise wake profile is taken per angle of attack, as has often been done in the past.

Introduction

IN recent years, considerable effort has been directed toward understanding the complex aerodynamics at low Reynolds numbers (Re). Attention in this area has increased because of the current need for the design and evaluation of efficient airfoil sections at chord Reynolds numbers from 1×10^5 to 1×10^6. Typical applications include unmanned aerial vehicles, wind turbines, sailplanes, ultralight aircraft, and high-altitude jet engine fan, compressor, and turbine blades.

To date, it is still very difficult to model low Reynolds number flow over airfoils where laminar separation and transition to turbulent flow is present because of the complex physics of laminar separation bubbles. As a result, wind-tunnel tests are often required. Unfortunately, in the typical low Reynolds number regime from 5×10^5 to 5×10^6, there are often large discrepancies between experimental results from different wind-tunnel facilities in both stall hysteresis behavior[1-4] and drag polar results[5-7] (Fig. 1). Possible explanations to account for this disparity of results include differences in model accuracy, freestream disturbance levels, data-acquisition techniques, wind-tunnel corrections, and the actual accuracy of the data.

Because of the extremely small drag forces on airfoils at low Reynolds numbers, profile drag is often best obtained by the momentum method instead of a force balance. Ideally, spanwise integration for calculating profile drag of airfoil sections should not be necessary since the flow is expected to be strictly two dimensional (except near the walls). In practice,

however, this assumption is false, especially at low Reynolds numbers.[8] Even at a Re as high as 1×10^6, Althaus[9] found aperiodic spanwise drag variations of approximately $\pm 15\%$, as shown in Fig. 2.

Although the occurrence of airfoil wake spanwise nonuniformity is well documented,[6,9-13] the phenomenon itself has received little in-depth attention, with a few exceptions. Flow visualization performed by Batill and Mueller et al.[14-17] showed that the wake of a NACA 66_3-018 airfoil was composed of large-scale vortices at $Re = 5.5 \times 10^4$. At an angle of attack of 8 deg, the laminar separation bubble does not form uniformly across the span, and the transition process is unsteady and three dimensional.[14] According to Mueller, these
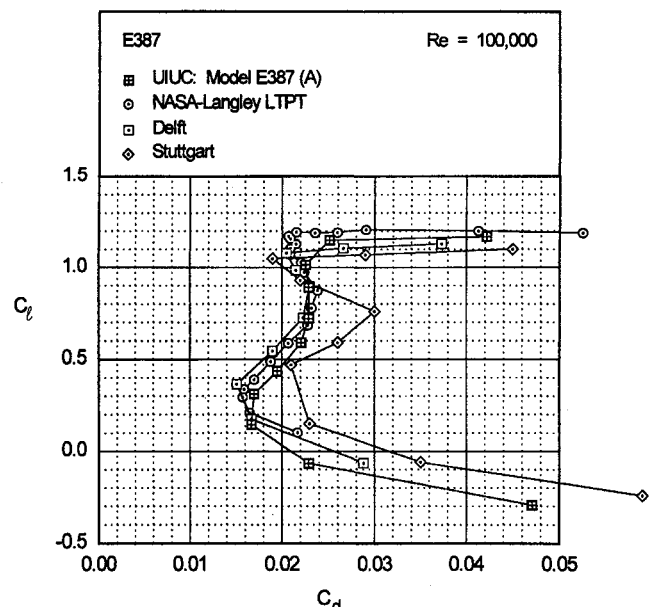

Fig. 1 Comparison of drag data for the E387 airfoil from the University of Illinois, NASA Langley LTPT,[6] Delft,[7] and Stuttgart[5] wind-tunnel facilities.

*Graduate Research Assistant; currently Engineer/Scientist, McDonnell Douglas Aerospace, 5301 Bolsa Avenue, Department A3-Y981, Building 13-3, Huntington Beach, CA 92647. Member AIAA.
†Assistant Professor, Department of Aeronautical and Astronautical Engineering, 306 Talbot Laboratory, 104 South Wright Street. Member AIAA.
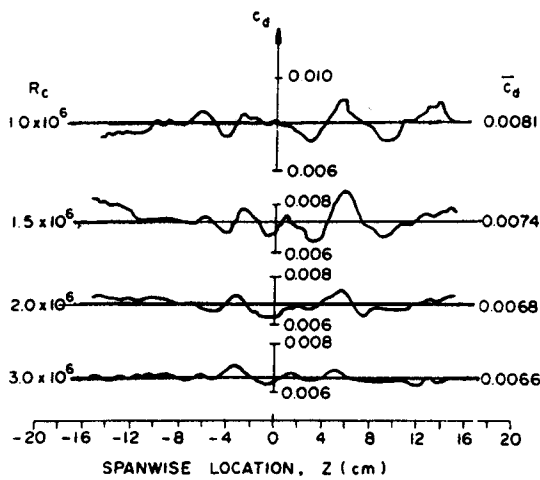
Fig. 2 Spanwise variation in profile drag coefficient at Reynolds numbers ranging from 1–3 × 10^6 (Mueller,[17] adapted from Althaus[9]).
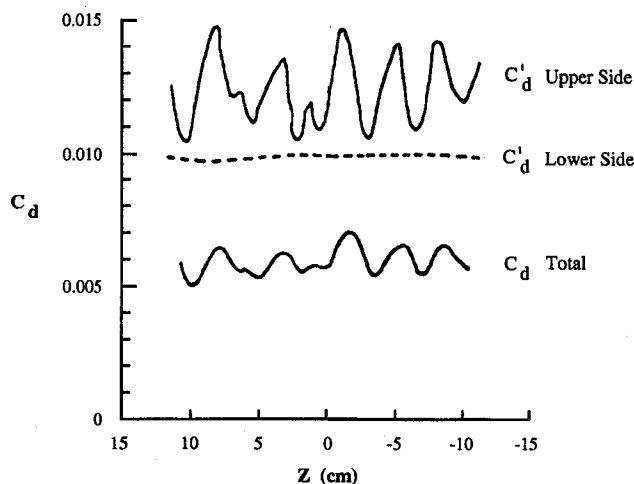

Fig. 3 Spanwise variation in profile drag for the FX 78-K-140 airfoil at $Re = 2.5 \times 10^6$ and $\alpha = 3$ deg. Wake traverses performed at trailing edge of model (adapted from Althaus[9]).

large-scale structures tend to produce an unsteady or oscillating wake similar to the wake behind a circular cylinder.

Boundary-layer measurements at higher Reynolds numbers (1–3 × 10^6) taken by Althaus[9] on different airfoil sections revealed that these flow structures are counter-rotating vortices that originate in the laminar separation bubble and result in the aperiodic spanwise variation in drag. This hypothesis was further verified by Althaus through wake traverses at the trailing edge of a FX 78-K-140 airfoil at an angle of attack of 3 deg and Re of 2.5 × 10^6. While the drag on the suction side of the airfoil showed periodic oscillations with a spatial wavelength of approximately 3 cm, the drag was fairly constant on the pressure side (Fig. 3). Unfortunately, no results were presented at negative angles of attack to see if the trend reversed. According to Althaus, the amplitudes of the variations depend on the curvature of the airfoil surface. Concave curvatures amplify the oscillations, whereas convex curvature has a damping effect. Althaus dismissed the notion that irregularities in the tunnel flow quality are the cause for the spanwise variations. After creating artificial disturbances by placing several 5-cm-wide rods behind the last screen in the contraction section of the tunnel, no oscillations in drag corresponding to these rods were generated.

More recently, work has been conducted on the three-dimensional structure of mixing layers and flat plate wakes in which spanwise variations in the mean streamwise velocity and

Reynolds stresses were observed.[18,19] These variations are believed to be linked to the formation of streamwise vortices in the initial laminar boundary layer. Results from this work may provide some clues to the presence of spanwise drag variations on airfoils.

Clearly, the intrinsic three-dimensional nature of the nominally two-dimensional flow at low Reynolds numbers creates opportunities for airfoil-performance measurement error, and this may explain the sometimes wide discrepancies between low Reynolds number airfoil data taken at different facilities. The reported drag data will depend on the location of the wake survey, or if multiple surveys are taken, the number of wake surveys and their locations. It is therefore important to have an indication of the anticipated degree of the spanwise drag variation. Thus, the objectives of this research were as follows:

1) Perform detailed spanwise drag measurements to document the character of the spanwise drag variations.
2) Examine the dependence of these variations to changes in the airfoil geometry, angle of attack, and Reynolds number.
3) Make recommendations on how to take accurate profile drag data through wake surveys in the Reynolds number range 2–5 × 10^5.

Experimental Facility

Research was conducted in the University of Illinois at Urbana–Champaign (UIUC) low-turbulence subsonic wind tunnel shown in Fig. 4. The wind tunnel is an open-return type with a 7.5:1 contraction ratio. The dimensions of the rectangular test section are nominally 2.8 × 4.0 × 8.0 ft, with the width increasing by approximately 0.5 in. over the length of the test section to account for boundary-layer growth along the tunnel side walls. Test-section speeds are variable up to 160 mph via a 125-hp ac electric motor connected to a five-bladed fan. At an airfoil chord $Re = 5 \times 10^5$, the resulting test-section speed was 80 ft/s (55 mph). To ensure good flow quality in the test section, the wind-tunnel settling chamber contains a 4-in.-thick honeycomb and four antiturbulence screens, which can be partially removed for cleaning. The empty test-section turbulence level is less than approximately 0.1% over the tunnel operating range.

The experimental setup is depicted in Fig. 5. For the current tests, the airfoil models were mounted horizontally between two 3/8-in.-thick, 6-ft-long Plexiglas® endplates (not depicted in Fig. 5 for clarity) to isolate the ends of the model from the tunnel side-wall boundary layers and the support hardware. Gaps between the model and Plexiglas were nominally 0.05 in. One side of the airfoil was free to pivot (far side of Fig. 5). At this location, the angle of attack was measured using an ac potentiometer (rotary transformer). The other side of the airfoil model was connected to the lift carriage through two steel wing rods that passed through the wing–rod fixture and were anchored to the model through two set screws. At this side, the airfoil model was free to move vertically on a precision ground shaft, but not free to rotate. A servo feedback-control force balance, however, restrained the motion of the model, as discussed later. Linear and spherical ball bearings within the lift carriage helped to minimize any frictional effects.

The two wind-tunnel models used for this investigation were the E374 and SD6060 airfoil sections. Both models have a
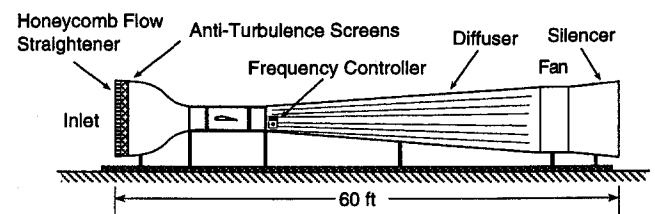

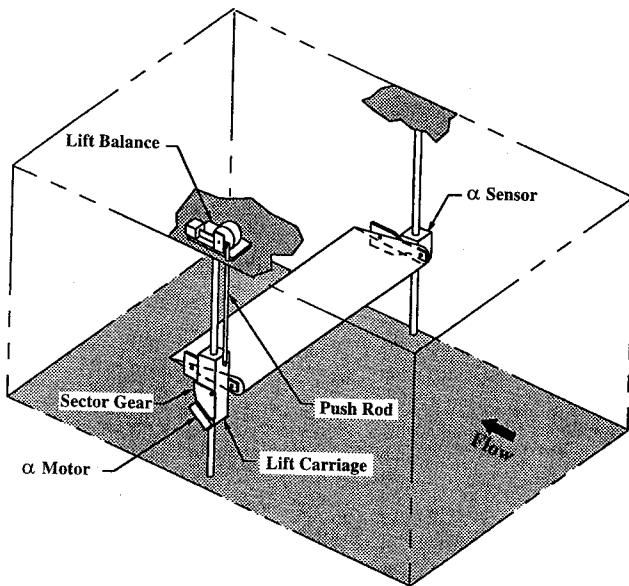Fig. 4 UIUC low-speed subsonic wind tunnel (not to scale).

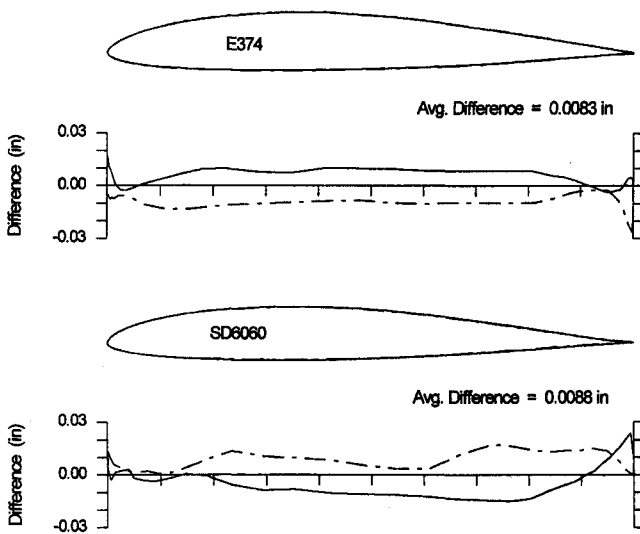**Fig. 5 Experimental setup (Plexiglas endplates and traverser not shown for clarity).**

Fig. 6 Section profile and model accuracy plots for the E374 and SD6060 airfoils.

foam core covered in an outer skin of fiberglass, with a 12-in. chord and $33\frac{5}{8}$-in. span ($\pm 1/64$ in tolerances). To determine the accuracy of the wind-tunnel models, each model was digitized using a Brown & Sharpe coordinate measuring machine to determine the actual airfoil shape. Approximately 80 points were taken about the airfoil with a spacing more or less proportional to the local curvature; near the leading and trailing edges the spacing was relatively small, whereas over the central section it was as large as 0.7 in. On average, the SD6060 and E374 were accurate to 0.009 and 0.008 in., respectively.

Section profiles and model accuracy plots are presented in Fig. 6. The profiles include both the true airfoil as designed (solid line) compared with the actual digitized model coordinates (dotted line). The model accuracy plots depict the differences between the nominal and actual coordinates for the upper surface (solid line) and lower surface (dotted line) of the airfoil. A displacement above or below the axis means that the model surface lies above or below the nominal, respectively. For instance, as seen in Fig. 6, the actual SD6060 wind-tunnel model was thinner than the true SD6060 by approximately 0.008 in. over the majority of the chord.

Measurement Techniques and Data Reduction

Lift Measurements

The wind-tunnel model was connected to the lift balance through a pushrod attached to the lift carriage, as shown in Fig. 5. The lift-force transducer was a servo balance rather than a standard strain gauge or load cell. Similar to a standard beam balance, the dead weight of the airfoil and support structure were counterbalanced with weights. The remaining forces (lift and residual imbalance) were then balanced by the torque from a brushless dc torque motor mounted on the beam axis. Any angular displacement from a reference zero was sensed by an ac potentiometer, and the error signal was used to drive the torque motor until the error disappeared. The lift balance was calibrated over the anticipated load range for a given run. Overall accuracy of the lift measurements is estimated to be 1.5%, based on the calibration results.

Drag Measurements

Profile drag was determined through the momentum method developed by Jones[20] (taken from Schlichting[21]) and is presented in detail in Ref. 22. To ensure that the wake had relaxed to tunnel static pressure, the wake measurements were performed 14.8 in. (≈ 1.25 chord lengths) downstream of the trailing edge of the airfoil. In some special cases, however, measurements were taken closer to the trailing edge. No static pressure corrections were applied to these measurements at the trailing edge since they were mainly qualitative in nature.

Two side-by-side pitot probes (spaced 3.96 in. apart in the spanwise x direction) were connected to the main traverser post that extended vertically through the tunnel test-section floor. The pitot probes had a rated accuracy of less than 1% error in total pressure for yaw and pitch angles less than 5 deg. The resolution and position accuracy of the traverser system is less than 0.001 and 0.005 in., respectively, in both the spanwise x direction and vertical y direction. Readout accuracy in the spanwise and vertical directions is 0.020 and 0.002 in., respectively.
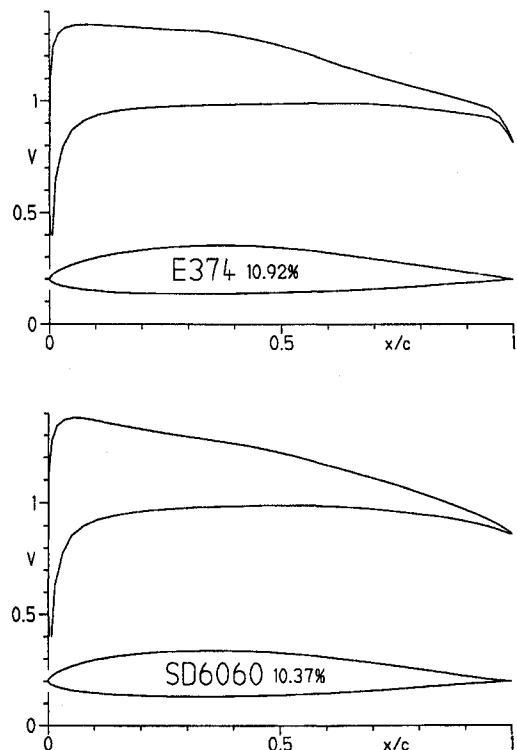

Fig. 7 Inviscid velocity distributions for the E374 and SD6060 airfoil sections at $C_l = 0.5$.
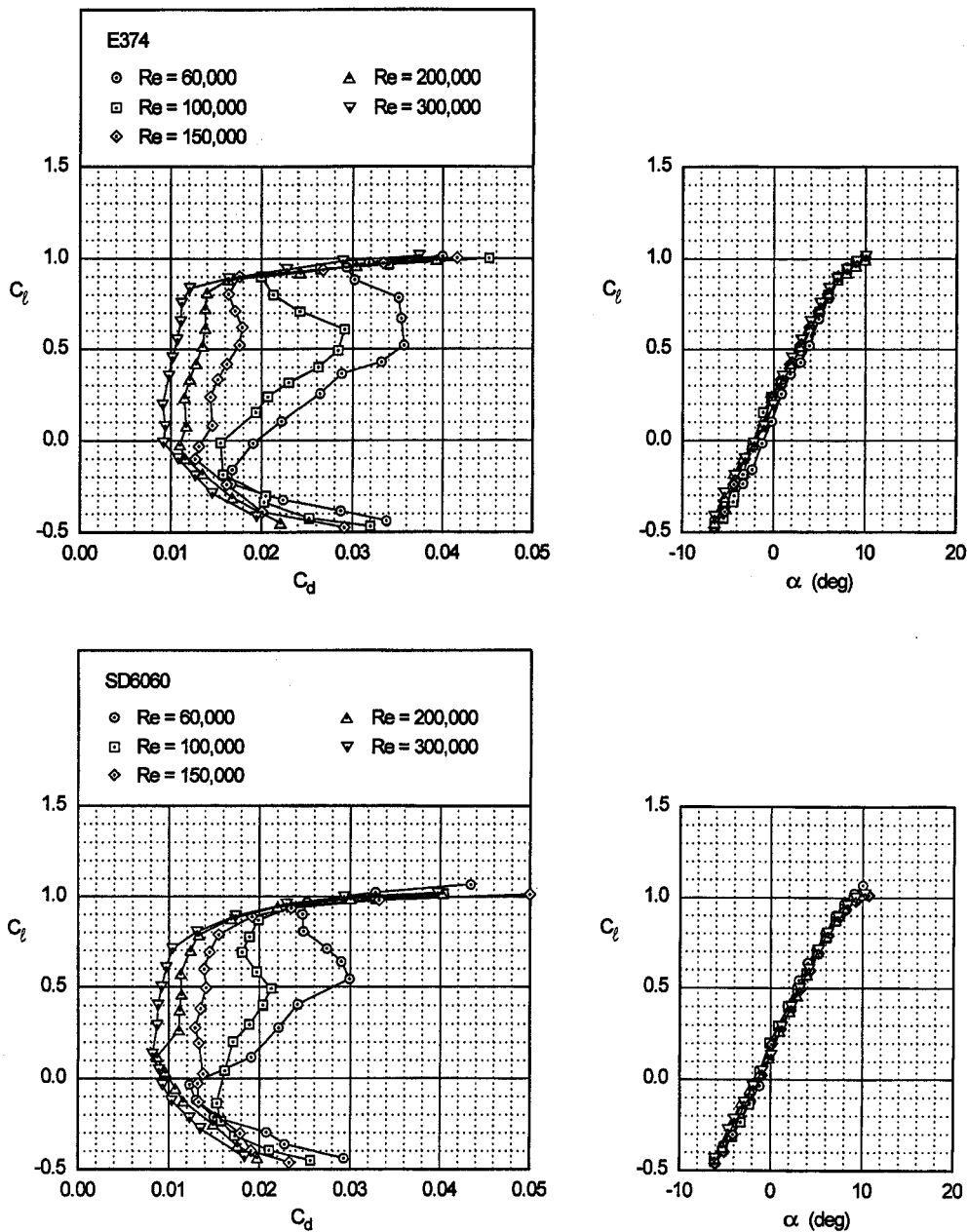
Fig. 8   Drag polars for the E374 and SD6060 airfoils.

Primary emphasis was placed on resolving the spanwise profile drag variations, and as a result, detailed vertical surveys through the wake were made at 57 spanwise stations nominally spaced 0.25 in. apart. Each vertical wake traverse consisted of between 20–80 total-head pressure measurements (depending on wake thickness) with points nominally spaced 0.08 in. apart. On average, a typical run involving 57 spanwise stations required 2 h of wind-tunnel operation.

Overlapping measurements by each probe were taken over the center 4.5 in. of the airfoil to obtain an estimate of the repeatability of the measurements. For all of the figures, the open-square symbols represent results from the first probe, and the black-diamond symbols represent results from the second probe. No measurements were taken in stall because of the size and unsteadiness of the wake.

Pressure measurements within the wake were made using MKS Baratron Model 220 variable-capacitance differential pressure transducers with a full-scale range of 1 mmHg (0.02 psia), resolution of 0.01% of full-scale reading and an accuracy of 0.15% of reading.

Data Acquisition and Reduction

All analog data were recorded on an AT&T 386 computer through a Data Translation DT2836 16-bit A/D data acquisition board. The DT2836 has a resolution of 0.0015% of full-scale reading, eight differential input channels, and two 16-bit D/A output channels. Set for a full-scale range of ± 10 V, the 16-bit resolution of the board provided an accuracy of ± 0.305 mV.

At the low speeds required for low Reynolds number tests, there were small time-dependent fluctuations in tunnel speed because of the inertia of both the drive system and the air. Thus, all quantities (dynamic pressure, total pressure, lift, angle of attack, x position, y position, and temperature) were measured simultaneously through a computer-controlled data-acquisition system. Once a run started, the entire data acquisition process was completely automated, including setting and maintaining a constant Reynolds number within the test section, acquiring data, and plotting raw data graphically to the computer screen and numerically to a printer. All data were also saved in a separate output file for later data reduction.
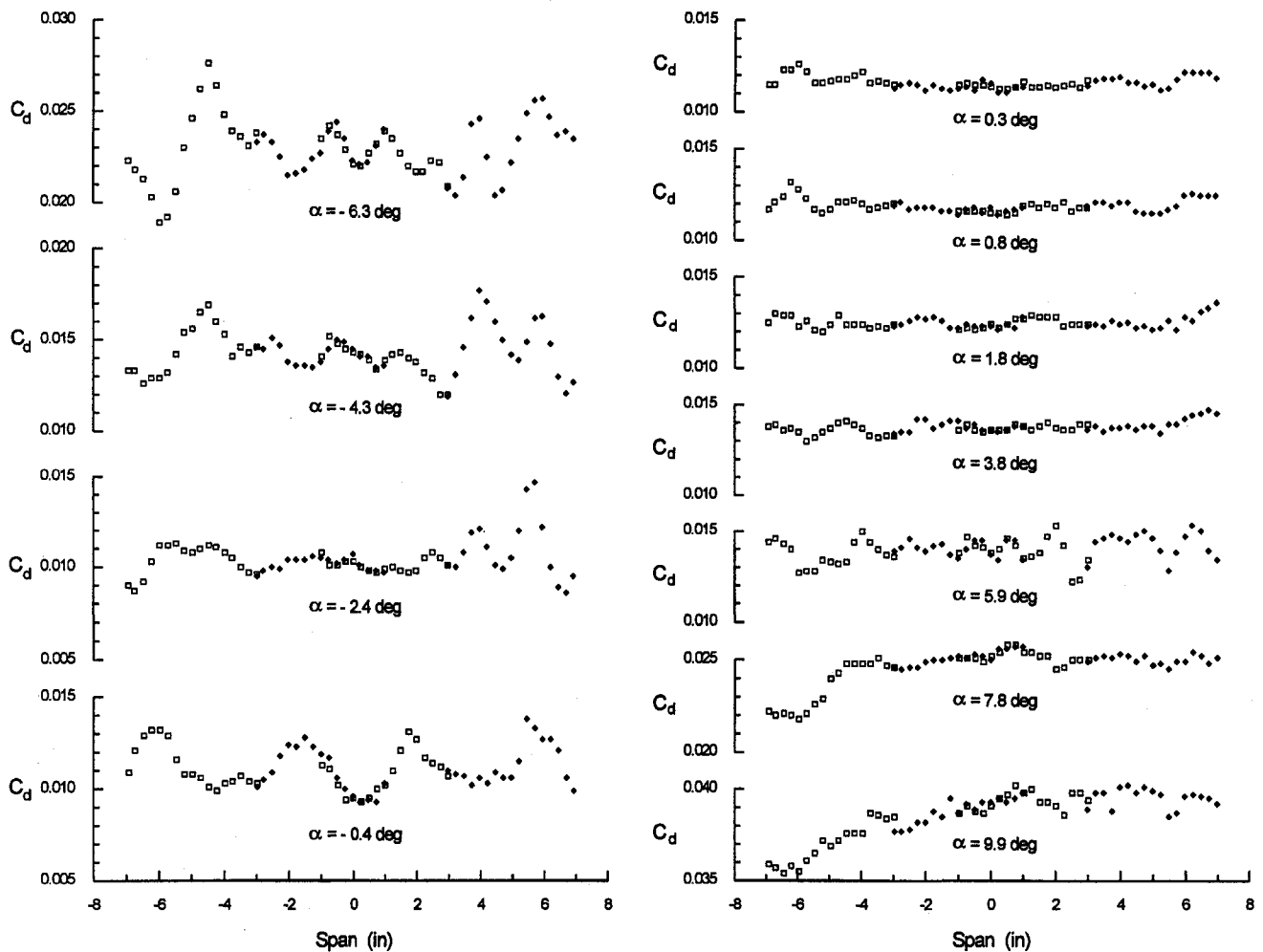
Fig. 9 Spanwise drag results for the E374 airfoil at $Re = 2 \times 10^5$.

Standard wind-tunnel corrections from Rae and Pope,[8] with slight modification to account for the presence of the endplates within the test section, were applied to the data. Further details concerning the blockage and velocity corrections are presented in Ref. 23. As documented in Ref. 23 and Fig. 1, data for the E387 are in good agreement with results from other facilities.

Results

For comparison of the performance of the E374 and SD6060 airfoils, velocity distributions (inviscid) and drag polars over a Reynolds number range from 6×10^4 to 3×10^5 are presented in Figs. 7 and 8, respectively. The SD6060 has considerably less drag than the E374, especially at low Reynolds numbers in the mid-to-high lift range. This difference in drag arises from the relatively strong pressure gradient along the upper surface of the E374, resulting in a large separation bubble and the corresponding high drag values. The SD6060 was designed to be an improvement over the E374 by making the velocity recovery along the upper surface more gradual.[7,24] The gradual pressure recovery is achieved by starting the recovery region farther upstream. The longer region of a smaller adverse pressure gradient is termed a bubble ramp, which when effectively employed, reduces the size of the separation bubble and lowers drag.

Figure 9 depicts the spanwise drag results at $Re = 2 \times 10^5$ for the E374 airfoil. Below an angle of attack of 0.3 deg, significant spanwise variations are present, with amplitudes deviating approximately 20% from the mean. Over the central 4.5 in. of overlapping measurements, the close agreement clearly indicates that the spanwise variation is a steady-state phenomenon. Further evidence of aperiodic behavior in the

spanwise drag at low Reynolds numbers is depicted at angles of attack of -6.3, -4.3, and -0.4 deg. At $\alpha = -6.3$ and -4.3 deg, the period (or spatial wavelength) of the variation is approximately 2 in., doubling to 4 in. at $\alpha = -0.4$ deg. Between an angle of attack of 0.3-7.8 deg, the amplitude of the variations decreases dramatically to 5-10% from the mean value. At and above an angle of attack of 7.8 deg, the spanwise drag appears skewed, which may be because of corner vortices developing at the juncture between the model and endplates at the high-lift conditions.

Over an angle-of-attack range at a constant Reynolds number, the extremum values (peaks and valleys) are not always in the same spanwise location. Moreover, when the drag is nearly constant over the spanwise range for certain conditions (e.g., $\alpha = 3.8$ deg), the drag does not remain constant over this region for all angles of attack. Thus, for accurate drag data, several measurements should be taken along the span, and the drag values from each traverse should then be averaged.

Spanwise drag results for the SD6060 airfoil are depicted in Fig. 10. Similar to the E374 results, significant spanwise variations are present at low angles of attack, and at high angles of attack the spanwise drag is once again skewed. The variations, however, are more periodic for the SD6060 when compared with the E374 and have higher amplitudes at moderate angles of attack. Also, at $\alpha = 0.03$ deg, the amplitudes differ from the average by approximately 45%, compared to only 20% for the E374. The spatial wavelength of the variations is not constant but, instead, varies from approximately 1.5 to 3 in. at $\alpha = -2$ and -4 deg to 2 in. at $\alpha = 0$ deg.

One factor contributing to the differences in amplitudes between the E374 and SD6060 airfoils at moderate-to-high an-
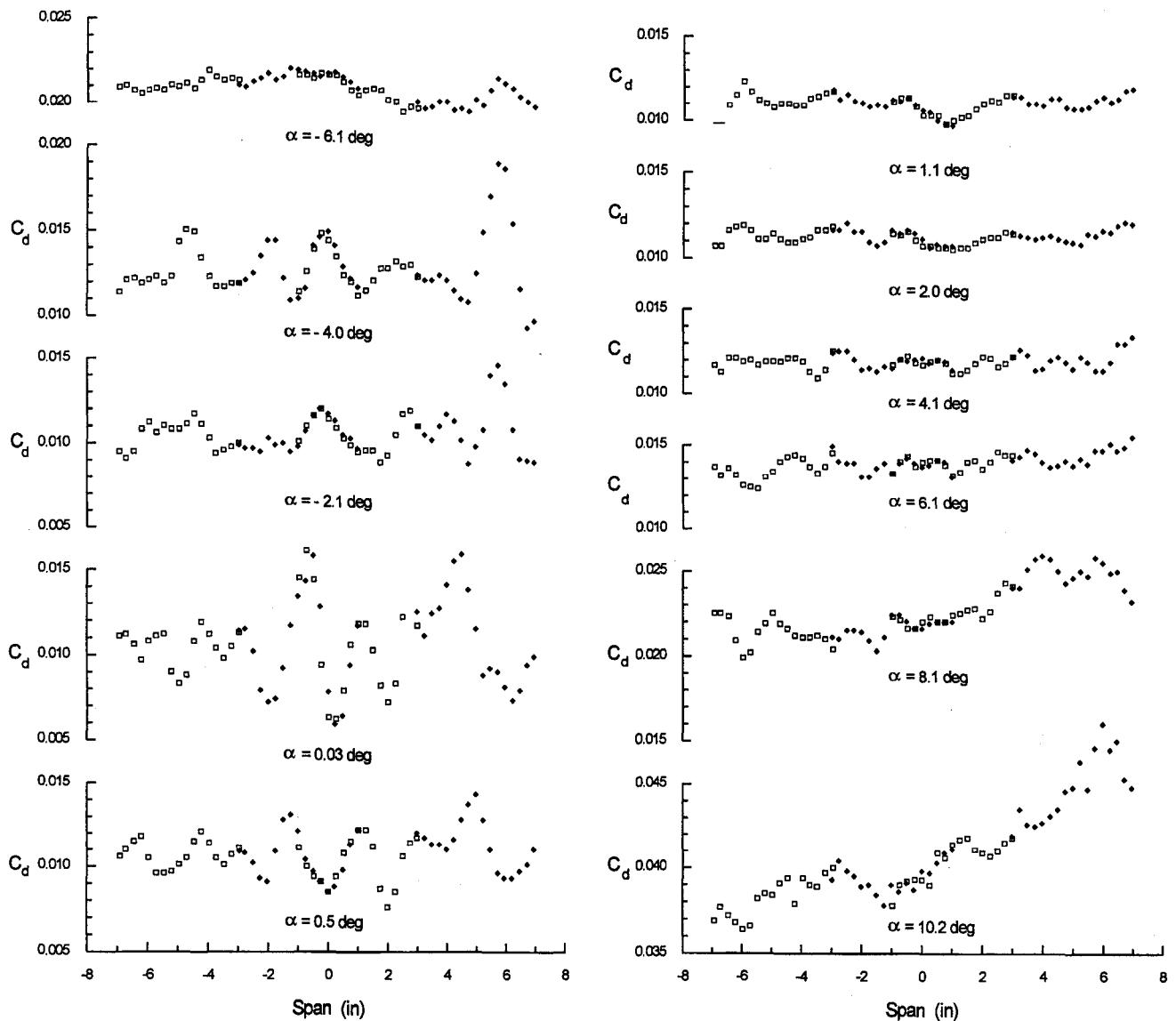
Fig. 10   Spanwise drag results for the SD6060 airfoil at $Re = 2 \times 10^5$.

gles of attack may be the type of the pressure recovery. Since the E374 has a steeper pressure recovery, the transition point and location of the separation may be more uniform across the model span, resulting in less spanwise drag variation compared with the SD6060 airfoil that has a more gradual upper surface pressure recovery.

For both airfoils, the largest drag variations occur below an angle of attack of 1 deg where the behavior of the laminar bubble on the lower surface of the airfoil may be a factor. At the low angles of attack that correspond to the lower limit of the low drag range (see Fig. 8), the laminar separation bubble moves forward relatively rapidly with decreasing angle of attack. As a result, some locations along the span on the lower surface may reach transition before other spanwise locations.

Reynolds number effects (up to $Re = 5 \times 10^5$) on the spanwise drag of the SD6060 airfoil are presented in Fig. 11 (points A and B are referred to later). The results indicate a significant Reynolds number dependence on the magnitude of the variations at and below a Re of 3×10^5. Above this value, the amplitudes remain fairly constant. Throughout the Reynolds number range investigated, the spanwise locations of the extremum values did not vary significantly with Reynolds number. Thus, while the Reynolds significantly affects the amplitude of the drag variations, it does not seem to have a great effect on the period and location of the variations.

To determine the effect of the airfoil wake, measurements were performed 0.2, 8.4, and 14.8 in. downstream of the trailing edge of the E374 (Fig. 12) and SD6060 (Fig. 13) airfoils. The angles of attack for each airfoil were selected as representative of extreme cases of spanwise profile drag variations. Since the wakes were thinner at the trailing edge (0.2 in.), the spacing between points within the wake was reduced to 0.05 in. for better resolution. Nevertheless, some of the scatter in the data at the trailing edge resulted from difficulties in resolving the relatively thin wakes. Since no static pressure corrections were applied to the data, the measurements at the trailing edge and 8.4 in. downstream are presented for qualitative comparisons only.

As the downstream distance from the trailing edge of the E374 is increased, the spanwise drag variations also increase. A similar result (at a different angle of attack) was obtained for the SD6060, except that some relatively large fluctuations were still present even at the trailing edge. These results indicate that the formation of the wake downstream of the airfoil plays a significant role in the magnitude of the spanwise variation.

Transition on the upper surface was fixed using a single strip of 0.019-in.-thick zigzag tape (Fig. 14) at the 20% chord location. At a Reynolds number of 2×10^5, no noticeable change in spanwise drag compared with the untripped case was
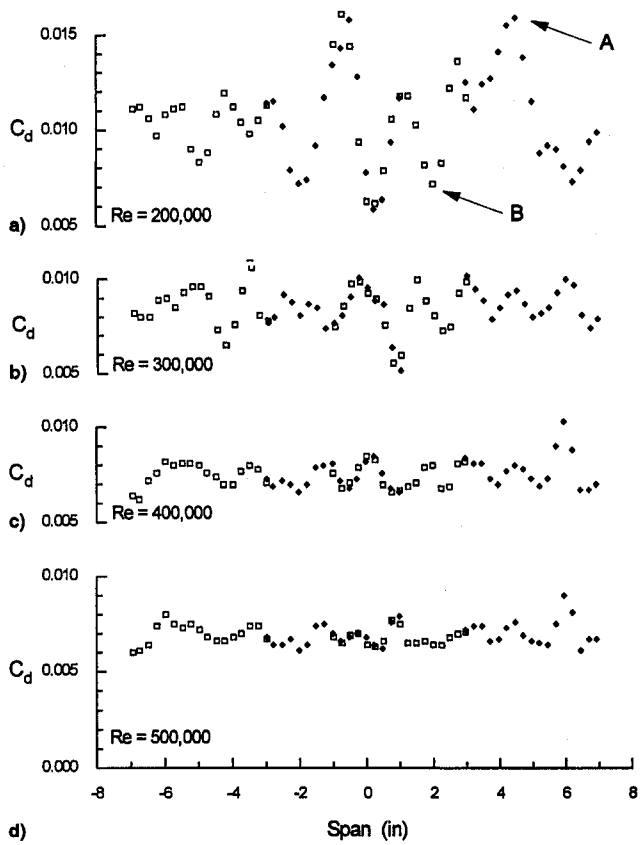
Fig. 11   Spanwise drag results for the SD6060 airfoil at 2 × 10^5 ≤ Re ≤ 5 × 10^5. α = a) 0.03, b) 0.09, c) 0.06, and d) 0.05 deg.
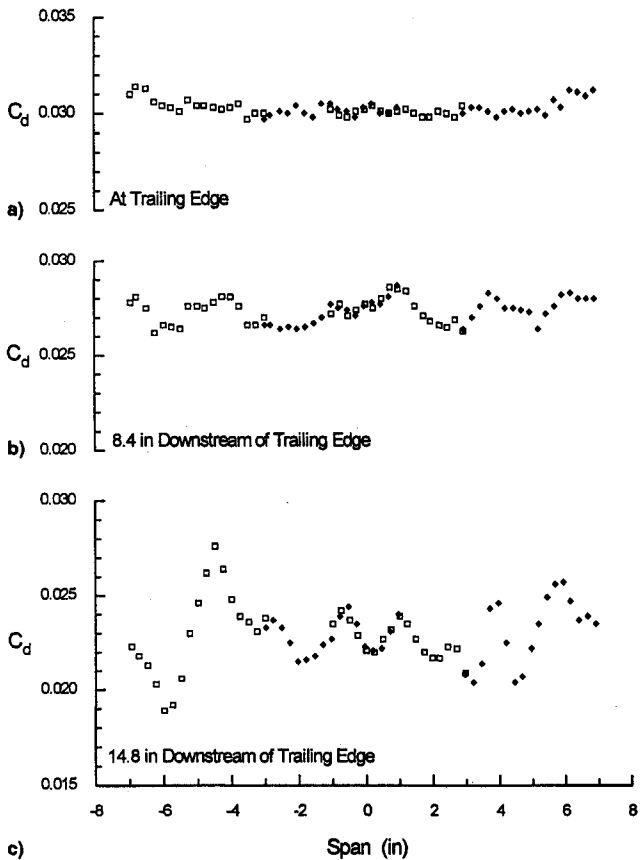

Fig. 12   Spanwise drag results at three locations downstream of the trailing edge of the E374 airfoil at a Reynolds number of 2 × 10^5. α = a) −6.4, b) −6.4, and c) −6.3 deg.
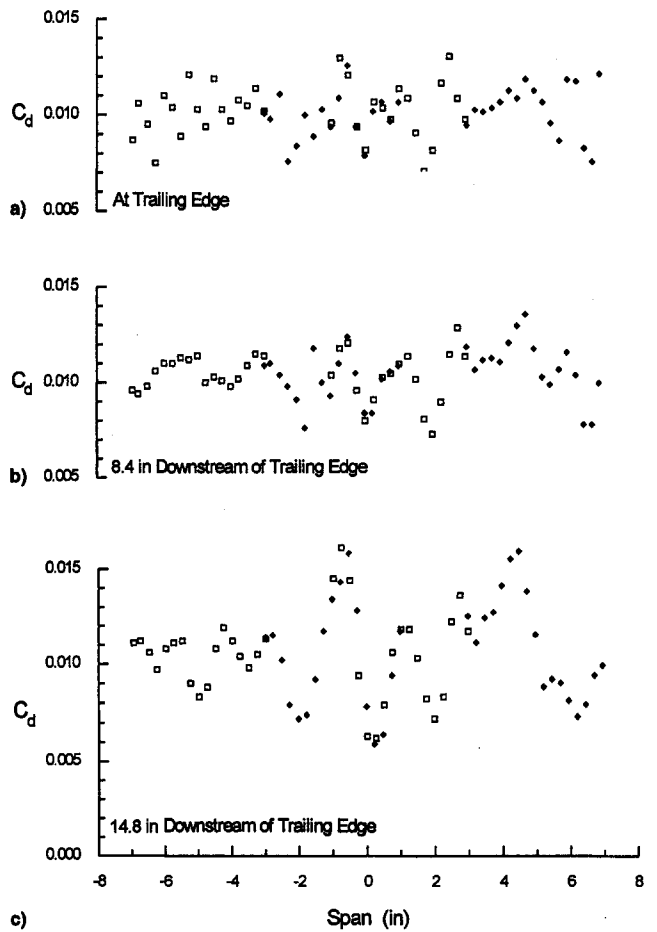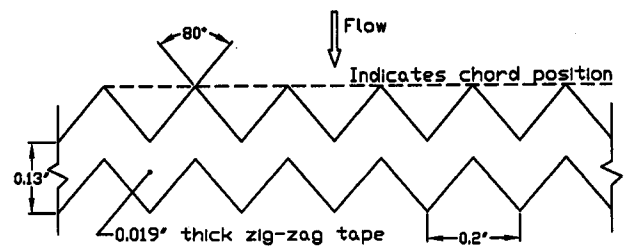

Fig. 13   Spanwise drag results at three locations downstream of the trailing edge of the SD6060 airfoil at a Reynolds number of 2 × 10^5. α = a) 0.02, b) −0.05, and c) 0.03 deg.
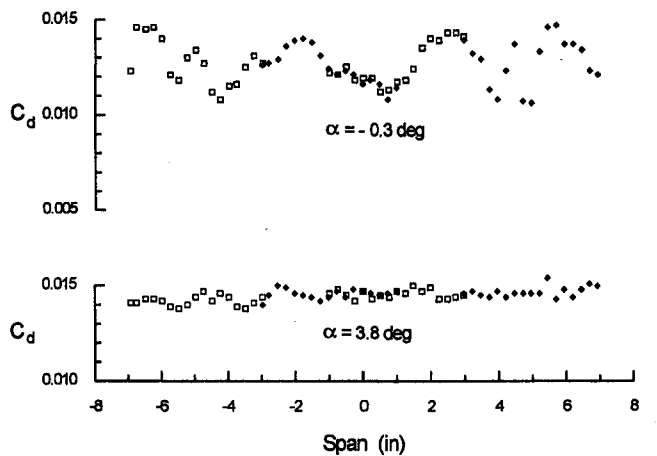

Fig. 14   Boundary-layer trip geometry.

Fig. 15   Spanwise drag results for the E374 airfoil with an upper surface trip.
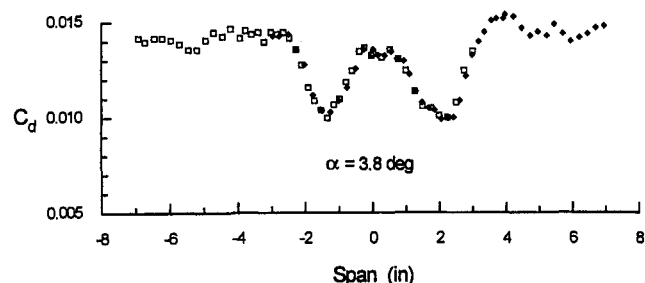
Fig. 16 Spanwise drag results for the E374 airfoil with a single hemisphere placed 0.2 in. behind the leading edge, centered with respect to the model span.
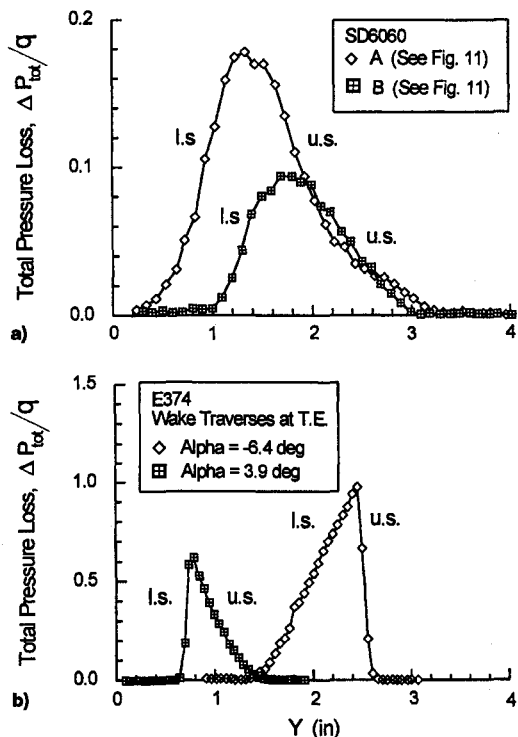

Fig. 17 Sample wake profiles for the a) SD6060 airfoil at $Re = 2 \times 10^5$, $\alpha = 0.03$ deg; and b) E374 airfoil at $Re = 2 \times 10^5$, $\alpha = -6.4$ and 3.9 deg.

found, as shown in Fig. 15. Since the average drag using the boundary-layer trips was higher than the clean configuration, the boundary layer was artificially tripped ahead of where the laminar separation bubble would otherwise occur. Since there are still spanwise variations at $\alpha = -0.3$ deg with early transition on the upper surface, it is clear that a laminar separation bubble on the upper surface is not the only source for the variations in drag.

An isolated hemisphere was centered on the upper surface of the E374 at 1.6% of chord to examine its effect on the downstream wake. The diameter and height of the hemisphere were 0.12 and 0.05 in., respectively. At a Reynolds number of 2×10^5 and an angle of attack of 3.8 deg, the single hemisphere induced a highly coherent drag variation that extended over the center 8 in. of the model span, as shown in Fig. 16. As would be expected, the perturbation in the profile drag is symmetrical and centered downstream of the hemisphere. When compared with the baseline data, the disturbance produced by the hemisphere is larger than that responsible for the natural variations in the profile drag.

Sample wake profiles for the SD6060 and the E374 airfoils are presented in Figs. 17a and 17b. The left and right sides of the wakes correspond to the airfoil lower surface (l.s.) and

upper surface (u.s.), respectively. Figure 17a depicts the wake profiles for the SD6060 at spanwise locations denoted by points A and B in Fig. 11. The wake corresponding to the high-drag spanwise location (point A) is almost double in magnitude compared to the wake profile for the low-drag location (point B). Wake profiles from traverses performed at the trailing edge of the E374 airfoil are depicted in Fig. 17b. At an angle of attack of 3.9 deg, almost all of the drag contribution comes from the upper surface, whereas the trend is reversed at an angle of attack of −6.4 deg.

Concluding Remarks

In an effort to document the peculiar drag characteristics of low Reynolds number airfoil flows, the nonuniformity of the airfoil profile drag along the span of several airfoils was investigated in detail. Several factors were found to influence the degree and character of the spanwise drag variation. The amplitudes of the oscillations decrease as the Reynolds number increases, which might indicate a dependence on the laminar separation bubble. The spanwise locations of the oscillations tend to shift with changes in the angle of attack, and the largest fluctuations occur at low angles of attack at the lower limit of the low drag range. This latter observation is most likely because of the behavior of the laminar separation bubble, which for this condition is known to move forward rapidly on the lower surface with decreasing angle of attack. Thus, the bubble is quite sensitive to the airfoil geometry and may not therefore be uniform across the model span because of model micro imperfections. The spanwise variations are also airfoil-shape dependent, which appear to be linked to the type of bubble ramp/pressure recovery employed. A more gradual ramp produces larger fluctuations. Finally, the wake downstream of the airfoil has a pronounced impact on the amplitudes of the spanwise drag; the amplitudes increase with distance downstream.

With spanwise drag variations often as high as 40% or more, it is not surprising that profile drag results determined by the momentum method can differ markedly depending on the test procedures implemented at a particular wind-tunnel facility. Thus, to ensure accurate profile drag measurements on airfoils at low Reynolds number by the momentum method, care must be taken so that the spanwise distance between wake surveys does not correspond to only peaks or valleys in the spanwise drag. Based on the current results, detailed vertical wake traverses spaced 2% of chord along the span is sufficient to ascertain the degree of the spanwise drag variations when measured 1.25 chord lengths downstream.

Acknowledgments

References

[1]Marchman, J. F., "Aerodynamic Testing at Low Reynolds Numbers," AIAA Paper 86-0779, March 1986.

[2]Mueller, T. J., "The Influence of Laminar Separation and Transition on Low Reynolds Number Airfoil Hysteresis," AIAA Paper 84-1617, June 1984.

[3]Mueller, T. J., Pohlen, L. J., Conigliaro, P. E., and Jansen, B. J., Jr., "The Influence of Free-Stream Disturbances on Low Reynolds Number Airfoil Experiments," Experiments in Fluids, Vol. 1, Springer–Verlag, New York, 1983, pp. 3–14.

[4]Schaefer, C. G., Jr., "Acoustic Effect on Stall Hysteresis for Low Reynolds Number Laminar Flow," AIAA Student Journal, Summer 1986, pp. 4–9.

[5]Althaus, D., Profilpolaren für den Modellflug—Windkanalmessungen an Profilen im Kritischen Reynoldszahlbereich, Neckar-Verlag Villingen-Schwenningen, Germany, 1980.

[6]McGhee, R. J., Walker, B. S., and Millard, B. F., "Experimental Results for the Eppler 387 Airfoil at Low Reynolds Numbers in the Langley Low-Turbulence Pressure Tunnel," NASA TM 4062, Oct. 1988.

[7]Selig, M. S., Donovan, J. F., and Fraser, D. B., *Airfoils at Low Speeds*, SoarTech 8, SoarTech Publications, Virginia Beach, VA, 1989.

[8]Rae, W. H., Jr., and Pope, A., *Low-Speed Wind Tunnel Testing*, Wiley, New York, 1984.

[9]Althaus, D., "Drag Measurements on Airfoils," OSTIV Congress, Paderborn, Germany, 1981.

[10]Awker, R. W., "The Design and Test of a Single Element Airfoil Optimized for High Lift," M.S. Thesis, Univ. of Illinois at Urbana–Champaign, Dept. of Aeronautical and Astronautical Engineering, Urbana, IL, 1974.

[11]Boermans, L. M. M., Duyvis, F. J. D., Van Ingen, J. L., and Timmer, W. A., "Experimental Aerodynamic Characteristics of the Airfoils LA 5055 and DU 86-084/18 at Low Reynolds Numbers," *Lecture Notes in Engineering: Low Reynolds Number Aerodynamics*, edited by T. J. Mueller, Vol. 54, Springer–Verlag, New York, June 1989.

[12]Boermans, L. M. M., and Van der Borne, P. C. M., "Design and Tests of a Flexible Sailwing Airfoil for Lightweight Aircraft," *Technical Soaring*, Vol. 12, No. 2, 1988.

[13]McGhee, R. J., and Walker, B. S., "Performance Measurements of an Airfoil at Low Reynolds Numbers," *Lecture Notes in Engineering: Low Reynolds Number Aerodynamics*, edited by T. J. Mueller, Vol. 54, Springer–Verlag, New York, June 1989.

[14]Batill, S. M., and Mueller, T. J., "Visualization of Transition in the Flow over an Airfoil Using the Smoke-Wire Technique," *AIAA Journal*, Vol. 19, No. 3, 1981, pp. 340–345.

[15]Mueller, T. J., and Batill, S. M., "Experimental Studies of Separation on a Two-Dimensional Airfoil at Low Reynolds Numbers," *AIAA Journal*, Vol. 20, No. 4, 1982, pp. 457–463.

[16]Mueller, T. J., and Jansen, B. J., Jr., "Aerodynamic Measurements at Low Reynolds Numbers," AIAA Paper 82-0598, March 1982.

[17]Mueller, T. J., "Low Reynolds Number Vehicles," AGARD, AGARDograph 288, Feb. 1985.

[18]Plesniak, M. W., Mehta, R. D., and Johnston, J. P., "Curved Two-Stream Turbulent Mixing Layers: Three-Dimensional Structure and Streamwise Evolution," *Journal of Fluid Mechanics*, Vol. 270, 1994, pp. 1–50.

[19]Weygandt, J. H., and Mehta, R. D., "Three-Dimensional Structure of Straight and Curved Plane Wakes," *Journal of Fluid Mechanics*, Vol. 282, 1995, pp. 279–311.

[20]Jones, B. M., "The Measurement of Profile Drag by the Pitot Traverse Method," British Aeronautical Research Council, R&M 1688, Jan. 1936.

[21]Schlichting, H., *Boundary Layer Theory*, McGraw–Hill, New York, 1979.

[22]Guglielmo, J. J., "Spanwise Variations in Profile Drag for Airfoils at Low Reynolds Numbers," M.S. Thesis, Univ. of Illinois at Urbana–Champaign, Dept. of Aeronautical and Astronautical Engineering, Urbana, IL, 1996.

[23]Selig, M. S., Guglielmo, J. J., Broeren, A. P., and Giguère, P., *Summary of Low-Speed Airfoil Data: Vol. 1*, SoarTech Publications, Virginia Beach, VA, 1995.

[24]Selig, M. S., and Donovan, J. F., "Low Reynolds Number Airfoil Design and Wind Tunnel Testing at Princeton University," *Lecture Notes in Engineering: Low Reynolds Number Aerodynamics*, edited by T. J. Mueller, Vol. 54, Springer–Verlag, New York, June 1989.